JOURNAL OF AGRICULTURAL AND FOOD CHEMISTRY

Optimization of Fabrication Parameters To Produce Chitosan−Tripolyphosphate Nanoparticles for Delivery of Tea Catechins

BING HU,[†] CHENLIANG PAN,[†] YI SUN,[†] ZHIYUN HOU,[§] HONG YE,[†] BING HU,[#] AND XIAOXIONG ZENG*,[†]

College of Food Science and Technology and Laboratory of Electron Microscopy, Nanjing Agricultural University, Nanjing 210095, People's Republic of China, and Malvern Instruments (China), Building 13 of Xinan Plaza, Tianzhou Road, Shanghai 200233, People's Republic of China

This work investigated the polyanion-initiated gelation process in fabricating chitosan−tripolyphosphate (CS-TPP) nanoparticles intended to be used as carriers for delivering tea catechins. The results demonstrated that the particle size and surface charge of CS-TPP nanoparticles could be controlled by fabrication conditions. For preparation of CS-TPP nanoparticles loaded with tea catechins, the effects of modulating conditions including contact time between CS and tea catechins, CS molecular mass, CS concentration, CS-TPP mass ratio, initial pH value of CS solution, and concentration of tea catechins on encapsulation efficiency and the release profile of tea catechins in vitro were examined systematically. The study found that the encapsulation efficiency of tea catechins in CS-TPP nanoparticles ranged from 24 to 53%. In addition, FT-IR analysis showed that the covalent bonding and hydrogen bonding between tea catechins and CS occurred during the formation of CS-TPP nanoparticles loaded with tea catechins. Furthermore, studies on the release profile of tea catechins in vitro demonstrated that the controlled release of tea catechins using CS-TPP nanoparticles was achievable.

KEYWORDS: Chitosan; chitosan−tripolyphosphate nanoparticles; controlled release; encapsulation; nanoparticle surface charge; nanoparticle size; tea catechins

INTRODUCTION

Tea, rich in catechins, is one of the most widely consumed beverages in the world. The principal catechins in tea leaves (*Camellia sinensis* L.) are (−)-epigallocatechin 3-gallate (EGCG), (−)-epicatechin 3-gallate (ECG), (−)-epigallocatechin (EGC), and (−)-epicatechin (EC). Tea catechins have received great attention due to their biological activities, such as antioxidant and antitumor activities (*1, 2*). On the other hand, the oral bioavailability of tea catechins is known to be low, <2−5% (*3, 4*). Due to strong systemic clearance, the half-life of tea catechins is short (*5*). It has been reported that the ingestion of tea catechins increased the antioxidant capacity of human plasma, whereas the concentration of tea catechins in plasma decreased rapidly (*6*). To resolve this problem, it is therefore essential to design an effective delivery system for tea catechins.

Chitosan (CS) is the deacetylated form of chitin and composed of glucosamine, known as 2-amino-2-deoxy-(1→4)-β-D-glucopyranan. It is considered to be the most widely distributed biopolymer as a cationic, nontoxic, biodegradable, and biocompatible polyelectrolyte. CS has been extensively investigated for its potential applications in the food, cosmetics, biomedical, and pharmaceutical fields (*7*). Due to their subcellular and submicrometer size, CS nanoparticles can penetrate deep into tissues through fine capillaries and cross the fenestration present in the epithelial lining. This allows efficient delivery of therapeutic agents to target sites in the body (*8–10*). For the preparation of CS nanoparticles, the ionotropic gelation method is commonly used. Under the acidic conditions, the $-NH_3^+$ protonized from $-NH_2$ of CS can interact with an anion such as tripolyphosphate to form microgel particles (*11, 12*). Ionic cross-linking of CS and tripolyphosphte (TPP) represents an advantageous method for preparing of drug-loaded nanoparticles because of its mild process of obtaining nanoparticles with a controlled size and satisfactory encapsulation capacity for macromolecules and drugs. In addition, reversible physical cross-linking by electrostatic interaction, instead of chemical cross-linking, makes it possible to prevent the toxicity of reagents and other undesirable effects (*10, 13*).

The physicochemical properties of nanoparticles are important in determining the physiological functions and stability of CS-TPP nanoparticles loaded with drugs. The particle size of

* Corresponding author (fax +86 25 84396791; e-mail zengxx@njau.edu.cn).
[†] College of Food Science and Technology, Nanjing Agricultural University.
[§] Malvern Instruments (China).
[#] Laboratory of Electron Microscopy, Nanjing Agricultural University.

10.1021/jf801111c CCC: $40.75 © 2008 American Chemical Society
Published on Web 07/16/2008

nanoparticles is one of the most significant determinants in mucosal and epithelial tissue uptake and intracellular trafficking (*14*). Surface charge is another important determinant in not only the stability, mucoadhesiveness, and permeation enhancing effect of the nanoparticles (*15, 16*) but also the ability of nanoparticles to escape from the endolysosomes (*17*). Some reports are found in the literature on controlling the fabrication parameters to modulate the physicochemical aspects of CS-TPP nanoparticles for the delivery of macromolecules such as genes and proteins in therapeutics (*10, 18, 19*). However, little information on CS nanoparticles loaded with bioactive polyphenolic antioxidant is available (*20*). The present study was therefore made to investigate the possibility of producing CS-TPP nanoparticles loaded with tea catechins by the ionotropic gelation method. Employing techniques such as particle size and zeta potential analysis, Fourier transform-infrared spectroscopy (FT-IR), transmission electron microscopy (TEM), and high-performance liquid chromatography (HPLC), we were able to examine effects of various preparation conditions on particle size, surface charge (zeta potential), polydispersity index (PDI), encapsulation efficiency, and release profile of tea catechins in CS-TPP nanoparticles.

MATERIALS AND METHODS

Materials. CS of five different molecular masses (30, 50, 100, 150, and 300 kDa), derived from crab shell was obtained from Golden-Shell Biochemical Co. Ltd. (Hangzhou, China). The degree of deacetylation was 90% for all. Folin−Ciocalteu reagent and sodium tripolyphosphate were purchased from Sigma-Aldrich. Product of tea catechins extracted from green tea was obtained from Nanjing Sorun Herbal Technology Development Co. Ltd. (Nanjing, China). The HPLC standards of EGCG, ECG, EGC, and EC were purchased from Funakoshi Co. Ltd. (Tokyo, Japan). All other chemicals were of analytical grade.

General Procedure for Preparation of Nanoparticles. CS-TPP nanoparticles were prepared according to the procedure reported previously (*18, 21*). Briefly, CS was dissolved in 1% (w/v) acetic acid solution with sonication until the solution was transparent. The aqueous solution of TPP was obtained at a concentration of 0.8 mg/mL. As a consequence of the addition of TPP solution to a CS solution with stirring at room temperature, the formation of CS-TPP nanoparticles started spontaneously via the TPP-initiated ionic gelation mechanism. For the preparation of CS-TPP nanoparticles loaded with tea catechins, the aqueous solution of tea catechins was added into CS solution for an appropriate time before the addition of TPP solution. The nanoparticle suspensions were immediately subjected to further analysis and applications.

Characterization of Nanoparticles. The morphological characteristics of nanoparticles were examined by a high-performance digital imaging TEM machine (JEOL H-7650, Hitachi High-Technologies Corp.). One drop of the suspension was stained with 2% (w/v) phosphotungstic acid, placed on a copper grid, and allowed to evaporate in air. Once evaporated, the samples were placed in a TEM for imaging. The accelerating voltage used was 100 kV, and the images were taken on a Gatan electron energy loss spectrometry system using a 6 eV energy slit.

The measurements of particle size, PDI, and zeta potential of nanoparticles were performed on a Zetasizer Nano-ZS (Malvern Instruments) on the basis of dynamic light scattering (DLS) techniques. FT-IR was carried out according to the potassium bromide pellet method on a Tensor-27 (Bruker) in the range of 500−4000 cm^{-1}.

Evaluation of Tea Catechin Encapsulation. CS-TPP nanoparticles loaded with tea catechins were carefully transferred into an Amicon Ultra-15 centrifugal filter device (Millipore Corp.) made up of a centrifuge tube and a filter unit with low-binding Ultracel membrane (10000 MWCO). After centrifugation at 4000*g* for 30 min, free tea catechins penetrated through the Ultracel membrane into the centrifuge tube, and the CS-TPP nanoparticles loaded with catechins in the filter unit were obtained and then freeze-dried by a Labconco Freeze-Dry System (Labconco Corp.). The ultrafiltrate in the centrifuge tube was collected for further analysis. The amount of tea catechins in ultrafiltrate was determined according to the Folin−Ciocalteu method (*22*). The encapsulation efficiency of tea catechins was calculated using the formula below:

$$\%\ \text{encapsulation efficienty} = \frac{\text{total amount of catechins} - \text{amount of catechins in ultrafiltrate}}{\text{total amount of catechins}} \times 100$$

In Vitro Release of Tea Catechins. The CS-TPP nanoparticles loaded with tea catechins obtained from the centrifugation were further used to determine in vitro release profiles of tea catechin. First, the nanoparticles in the filter unit were diluted by deionized water to 2.0 mL. Then the filter unit was sealed and placed in a water bath with the temperaature maintained at 37 °C. At specified collection times, the filter unit was placed back into the Amicon Ultra-15 centrifugal filter device and centrifuged at 4000*g* for 30 min. The nanoparticles in the filter unit were treated repeatedly as described elsewhere above. The amount of tea catechins in each ultrafiltrate was determined by HPLC as we previously described (*23*). The total released tea catechins mass M_i at time i was calculated using the formula

$$M_i = C_i V_i + \Sigma C_{i-1} V_{i-1}$$

where C_i is the concentration of one kind of tea catechins in the ultrafiltrate at time i and V_i is the ultrafiltrate volume.

Statistical Analysis. All experiments and analyses were performed in triplicate. The data were compared by one-way analysis of variance (ANOVA) using the SAS Software for Windows V8. The significant difference ($P < 0.01$) between sample means was further determined by Duncan's multiple-range test.

RESULTS AND DISCUSSION

Preparation of CS-TPP Nanoparticles. CS-TPP nanoparticles can easily be prepared upon the mixing of TPP solution with CS solution under stirring, because the obtainment of nanoparticles is based on an ionic gelation technique between positively charged CS and negatively charged TPP. It is noteworthy that many researchers have explored the capacity of CS-TPP nanoparticles to associate peptides, proteins, oligonucleotides, and plasmids DNA for potential pharmaceutical applications. As the physicochemical features of CS-TPP nanoparticles may affect the stability as a result of stable ionic interactions and biological performance of nanoparticles loaded with target molecules, it is important to elucidate the effect of preparation conditions on particle size or stability of CS-TPP nanoparticles. Therefore, we investigated the effects of CS molecular mass, CS concentration, CS-TPP mass ratio, and initial pH value of CS solution on particle size, PDI, and surface charge of CS-TPP nanoparticles before studying the fabrication parameters for CS-TPP nanoparticles loaded with tea catechins.

Effect of CS Molecular Mass. Figure 1A shows the influence of CS molecular mass on the particle size and PDI of the CS-TPP nanoparticles. There was no noticeable difference ($P > 0.01$) among the particle sizes when three CS molecular masses of 50, 100, and 150 kDa were used. However, the particle size decreased from 201.4 to 169.0 nm ($P < 0.01$) as the CS molecular mass increased from 30 to 50 kDa, and it rebounded to 309.7 from 173.3 nm ($P < 0.01$) in correspondence to the increase of CS molecular mass from 150 to 300 kDa. This phenomenon may be related to the shearing degradation of CS during the magnetic stirring of the mixture of CS and TPP (*19*). The mechanism of polymer shearing degradation is proposed as the polymer sheared along the direction of shearing flow; as a consequence, the strong elongated flow encountered

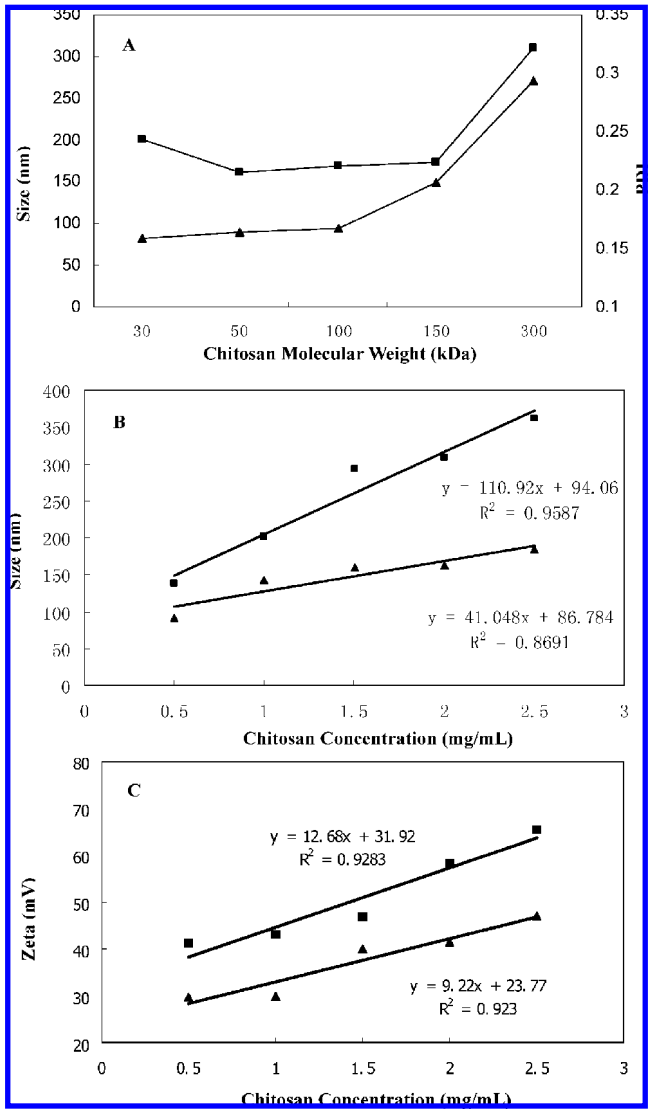

Figure 1. Effect of CS molecular masses from 30 to 300 kDa on particle size (■) and polydispersity index (▲) of CS-TPP nanoparticles (**A**). (CS concentration = 1.5 mg/mL; CS-TPP mass ratio = 6:1; pH 4.5.) Effect of CS concentration from 0.5 to 2.5 mg/mL on particle size (**B**) and zeta potential (**C**) of CS-TPP nanoparticles (CS molecular mass = 50 (▲) and 300 (■) kDa; CS-TPP mass ratio = 6:1; pH 4.5).

by the polymer may bring sufficient energy to disrupt the molecules. The shear stress to which the polymer is exposed exceeds a critical value specific to the polymer (*19, 24*). Therefore, the polymer has to be long enough to be entangled and stretched by the shearing force. It can be presumed that the length of the 30 kDa CS molecule is not long enough to be sheared to degrade into small fragments engaged in the formation of CS-TPP nanoparticles.

The PDI of CS-TPP nanoparticles increased from 0.164 to 0.294 in correspondence to the increase of CS molecular mass from 30 to 300 kDa, and all of the values of PDI were below 0.3. The results indicate that a homogeneous dispersion of CS-TPP nanoparticles is obtained. However, the heterogeneity became higher and higher as CS molecular mass increased, which may also be related to the polymer shearing degradation. The CS with high molecular mass is likely to be degraded to various fragments with different dimensions, which led to the obtained nanoparticle being more heterogeneous.

The same trend as the particle size and PDI changes as a function of the molecular mass could also be observed in the change in surface charge of the CS-TPP nanoparticles (data not shown). The chitosans with different molecular masses (degree of deacetylation = 90%) should have different available cationic groups, the higher molecular mass having more available cationic groups, resulting in the higher surface charge. These results are similar to those obtained by Gan et al. (*10*) and Wu et al. (*25*).

Effect of CS Concentration. Figure 1B shows the effect of CS concentration on the particle size at two different CS molecular mass values, 50 and 300 kDa. The particle size increased linearly with the increase of CS concentration within the experimental range. The particle size rose sharply accompanied by an increase in CS concentration at the molecular mass of 300 kDa. A similar result has been reported by Grenha et al. (*26*), who showed that a higher concentration of CS solution formed larger sized particles. A similar trend was observed in the change of PDI with the increase of CS concentration (data not shown), indicating that the homogeneity of CS-TPP nanoparticles became weaker as the CS concentration increased.

Figure 1C shows the effect of CS concentration on the zeta potential of CS-TPP nanoparticles. Within the tested range, the zeta potential of CS-TPP nanoparticles increased linearly with CS concentration. It is known that the formation of CS-TPP nanoparticles is based on the interaction between the protonized $-NH_3^+$ in CS and the polyanionic phosphate groups in TPP. The surface charge of the CS-TPP nanoparticles is determined by the degree of neutralization of $-NH_3^+$ by the polyanionic phosphate groups. At the same degree of deacetylation, the higher CS concentration means more total available $-NH_3^+$ in CS molecules. Compared with low CS concentration, there may be more unneutralized $-NH_3^+$ on the surface of nanoparticles formed with high CS concentration. Therefore, the zeta potential should increase with the increase of CS concentration. In addition, the larger nanoparticle size and higher PDI at higher CS concentration may also contribute to the higher amount of unneutralized $-NH_3^+$. More unneutralized $-NH_3^+$ led to stronger intramolecular repulsion, making the CS chain stretch to result in larger nanoparticles. However, Gan et al. (*10*) reported that the zeta potential of CS-TPP nanopaticles decreased with increasing CS concentration, which may be due to the differences in molecular masses and deacetylation degrees of the CS used.

Effect of CS-TPP Mass Ratio. CS-TTP mass ratio is another important factor influencing the characteristics of the formed CS-TPP nanoparticles. Gan et al. (*10*) reported that the particle size and the zeta potential increased linearly with the increasing CS-TPP mass ratio. However, an opposite trend in particle size was found in the present study. As shown in **Figure 2A**, the particle size decreased linearly with the increasing CS-TPP mass ratio. A similar result has been reported lately that the particle size declines as the CS-TPP mass ratio increases from 2:1 to 5:1 (*28*). It was observed that the formed nanoparticle suspension became more and more turbid as the CS-TPP mass ratio declined. Even opalescent floccules occurred when the CS-TPP mass ratio declined to 1.5:1, indicating the formation of large particles. A similar phenomenon has been reported that aggregates with large diameter are formed when the CS-TPP mass ratio is down to 1.25:1 (*25, 27*). It is known that the ability of CS to quickly gel on contact with TPP relies on the formation of inter- and intramolecular cross-linking between the amino groups and the phosphate groups. When the CS-TPP mass ratio was high (the available quantity of TPP was small), TPP might dominantly inter- and intramolecular cross-link with CS to form

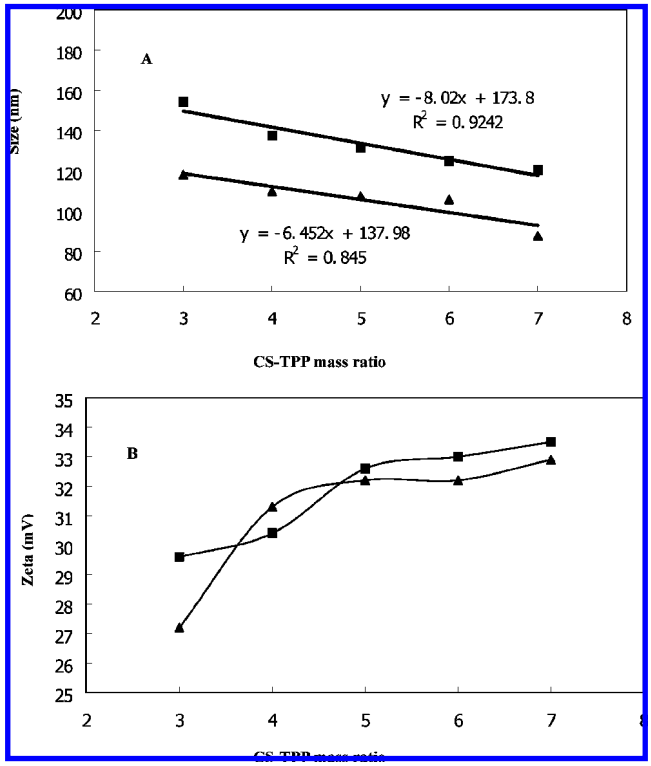

Figure 2. Effect of CS-TPP mass ratio on particle size (**A**) and zeta potential (**B**) of CS-TPP nanoparticles. [CS molecular mass = 50 kDa; CS concentration = 0.5 (▲) and 1.5 (■) mg/mL].

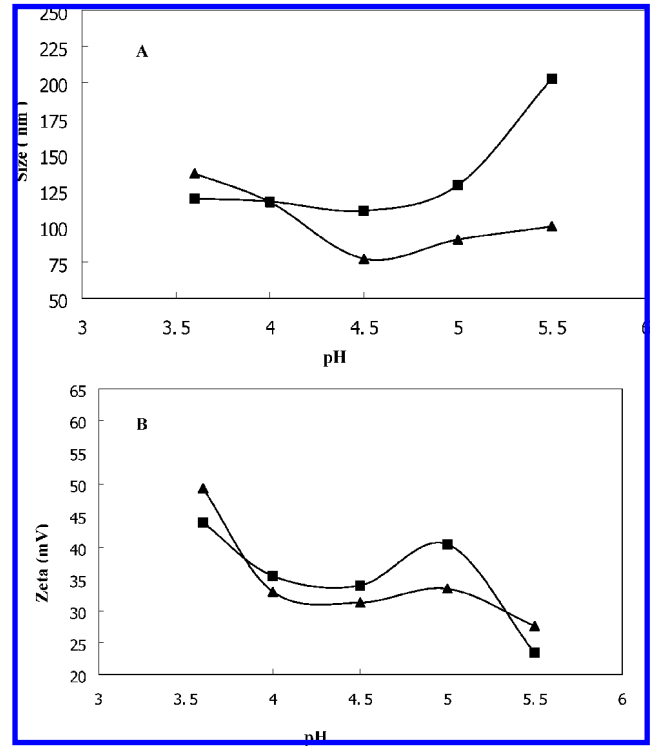

Figure 3. Effect of the initial pH values of CS solution on particle size (**A**) and zeta potential (**B**) of CS-TPP nanoparticles. [CS molecular mass = 50 kDa; CS concentration = 0.5 (▲) and 1.5 (■) mg/mL].

small monoparticles. As the CS-TPP mass ratio declined, the available quantity of TPP increased accordingly, and the superfluous TPP would link the monoparticles to form larger nanoparticles. This may also be confirmed by the changes in zeta potential and PDI of CS-TPP nanoparticles. As shown in **Figure 2B**, the zeta potential decreased sharply as the CS-TPP mass ratio decreased from 5:1 to 3:1, which might be caused by the screening of cation on the particle surface during the linkage or aggregation of the nanoparticles. On the other hand, a slow increase in zeta potential was observed as the CS-TPP mass ratio increased from 5:1 to 7:1, which might be due to less neutralization of the protonated amino groups in CS accompanied with less ionic cross-linking. In addition, the PDI of the nanoparticle suspension increased as the CS-TPP mass ratio declined from 7:1 to 3:1 (data not shown), which might be caused by the formation of the linkage or aggregation of the nanoparticles.

Effect of Initial pH Value of CS Solution. As a weak base polysaccharide, CS is insoluble at neutral and alkaline pH solutions. However, when it is dissolved in acidic medium, usually in 1% or 0.1 M acetic acid, the solubilization occurs by protonation of the $-NH_2$ group on the C-2 position of the D-glucosamine repeat unit, whereby the polysaccharide is converted to a polyelectrolyte in acidic media. Therefore, the ionic cross-linking process for the formation of CS-TPP nanoparticles is pH-dependent, providing opportunities to modulate the formulation and properties of CS-TPP nanoparticles.

To study the effect of the initial pH value of the CS solution on particle size and zeta potential, CS-TPP nanoparticles prepared with 50 kDa CS at a fixed CS-TPP mass ratio of 5:1 at two different CS concentrations (0.5 and 1.5 mg/mL) were examined at different pH values of CS solution. The variations in particle size and zeta potential with the pH value of the CS solution are shown in **Figure 3**. Both the smallest particle sizes and the lowest zeta potentials occurred at pH 4.5 for both CS concentrations used. The particle size and zeta potential decreased as the pH value increased from 3.6 to 4.5. Afterward, the particle size increased as the pH value rose from 4.5 to 5.5, but the zeta potential first increased as the pH rose to 5.0 and then decreased again as the pH increased to 5.5. A similar trend was also reported in another research paper (*13*). Below pH 4.5, the stronger protonation of the $-NH_2$ moiety led to a higher zeta potential and a stronger intramolecular repulsion, making the CS chain stretch and resulting in larger nanoparticles. Up to pH 4.5, the comparatively weak interaction between CS and TPP led to the formation of larger nanoparticles (*20*). As the pH value rose to 5.0, the relatively noncompact cross-linking between CS and TPP caused less neutralization of the $-NH_3^+$ group, resulting in the rise of the zeta potential. However, the protonation of the $-NH_2$ at pH 5.5 in CS molecules was essentially so weak that the zeta potential declined sharply.

Characterization of CS-TPP Nanoparticles. Figure 4A shows the morphological characteristic of CS-TPP nanoparticles by TEM image. CS-TPP nanoparticles were regularly spherical in shape. **Figure 4B** shows a typical size distribution profile of the nanoparticles with a mean diameter of 128.5 nm in a narrow size distribution (PDI = 0.185). Particle charge is a stability-determining parameter in aqueous nanosuspensions. Generally, a zeta potential of ±30 mV is required as a minimum for a physical stable nanosuspension solely stabilized by electrostatic repulsion (*29*). The zeta potential of the CS-TPP nanoparticles prepared in the present study was about +42.5 mV (**Figure 4C**).

Encapsulation Efficiency and Release of Tea Catechins. CS-TPP nanoparticles loaded with tea catechins were prepared according to a procedure similar to that used for the preparation of CS-TPP nanoparticles. From the extensive ongoing research in protein encapsulation in CS nanoparticles, it is possible to modulate the protein encapsulation efficiency and release rate by adjusting CS molecular mass, concentration of protein or

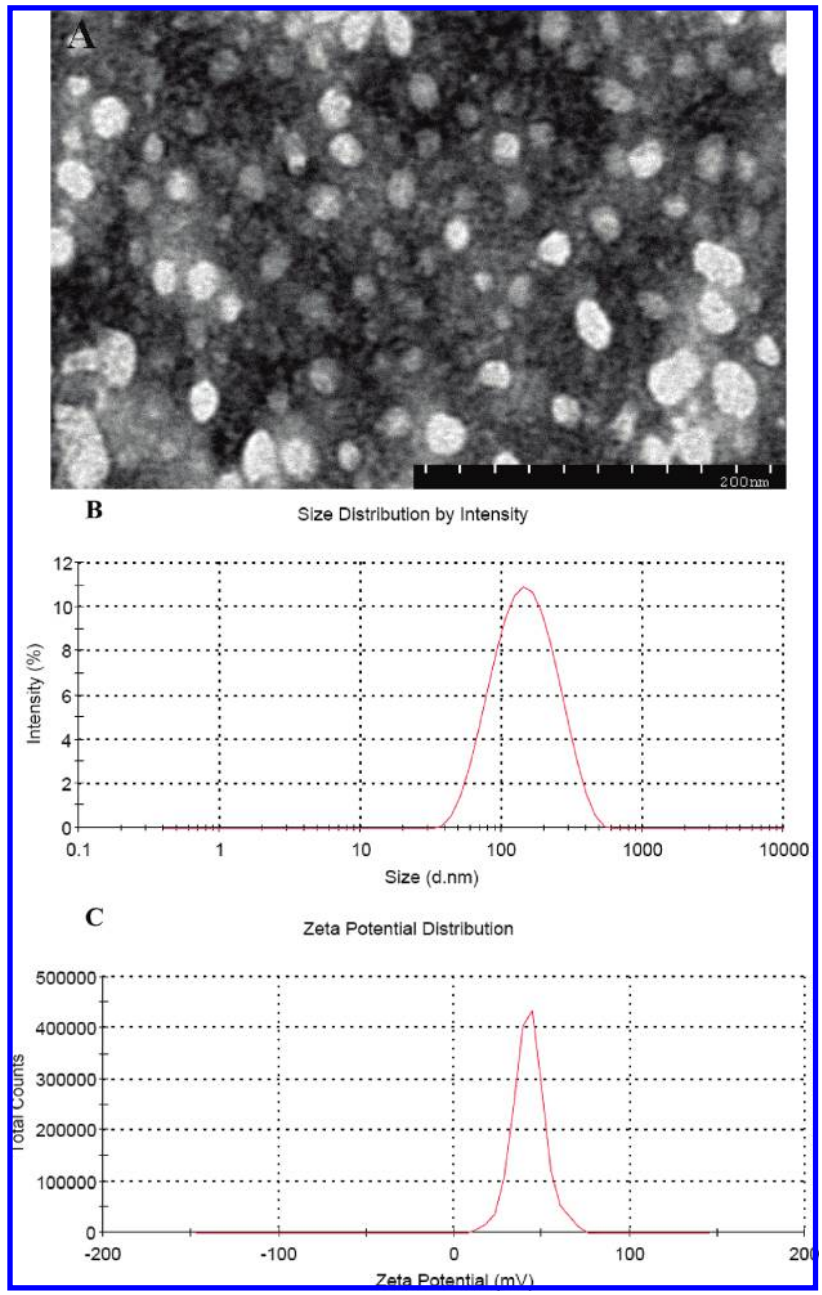

Figure 4. Characteristics of CS-TPP nanoparticles: (**A**) TEM image of CS nanoparticles; (**B**) size distribution; (**C**) zeta potential distribution.

CS, and CS-TPP mass ratios as well as the concentration of the ionic cross-link agent. However, studies on encapsulation efficiency and release are relatively few for the case of polyphenol as a target molecule (*20*). Therefore, we investigated the effects of modulating conditions (contact time between CS and tea catechins, CS molecular mass, CS concentration, CS-TPP mass ratio, initial pH value of CS solution, and concentration of tea catechins) on encapsulation efficiency and release in vitro of tea catechins of CS-TPP nanoparticles loaded with tea catechins.

Effect of Contact Time between CS and Tea Catechins. The highest encapsulation efficiency of tea catechins appeared after the mixture of tea catechins and CS was gently stirred for 30 min before the addition of TPP solution (data not shown). As we can see from the results of FT-IR (**Figure 5**), the covalent bonding and hydrogen bonding between tea catechins and CS occurred during the formation of nanoparticles loaded with tea catechins. Therefore, it can be presumed that the encapsulation efficiency of tea catechins should be time-dependent for the full interaction between tea catechins and CS. Therefore, all of the following mixtures of tea catechins and CS for studying encapsulation efficiency were gently stirred for 30 min before the addition of TPP solution.

Effect of CS Molecular Mass. Figure 6A shows that the encapsulation efficiency of tea catechin tended to increase from 25.84 to 47.37% and then to decrease to 35.95% in correspondence to the CS molecular mass increasing from 50 to 150 kDa and to 300 kDa, respectively, at the CS concentration of 1.5 mg/mL. The effect of CS molecular mass on the encapsulation efficiency may be in correlation with the different spread length of CS chain in the solution. For CS molecular masses of 50 and 150 kDa, the molecular chain should be fully extended in the solution at pH 4.5 because of the electrostatic repulsion between protonized amine groups presented along the molecular chain. The extended CS chains might offer more reactive sites for the formation of hydrogen bonds with tea catechins. Therefore, the tea catechin encapsulation efficiency increased as the molecular mass went up from 50 to 150 kDa.

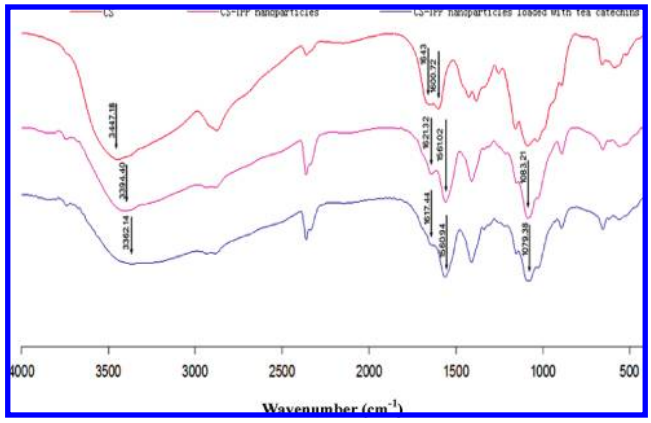

Figure 5. FT-IR spectra of CS, CS-TPP nanoparticles, and CS-TPP nanoparticles loaded with tea catechins.

However, when the molecular mass was up to 300 kDa, the encapsulation efficiency of tea catechins declined, possibly due to the steric hindrance caused by the bend and intertwist of the much longer spread chain.

In correspondence with the encapsulation efficiency, studies on tea catechin release in vitro showed that both the release kinetics and the total release of tea catechins at isothermal conditions (37 °C) first increased as the molecular mass increased from 50 to 150 kDa and then decreased when the molecular mass increased to 300 kDa (**Figure 6B**). It has already been reported that the release rate is usually drug concentration gradient driven (*27*). A high quantity of loaded tea catechins led to a wide concentration gap between CS-TPP nanoparticles and the release medium, which caused a high release rate. Therefore, the release rate varied according to the different encapsulation efficiencies. There was a dramatic reduction in tea catechin release after 12 h, and further release of tea catechins required the swelling and degradation of the compact CS-TPP nanoparticles. Hence, the results indicate that the CS-TPP nanosystem is suitable for controlling the release of tea catechins.

Effect of CS Concentration. The encapsulation efficiency of tea catechins increased linearly with the increase of CS concentration (**Figure 6A**). It has been reported that the encapsulation efficiency of bovine serum albumin (BSA) in CS-TPP nanoparticles decreased with increasing CS concentration, which was caused by the higher viscosity in the case of higher CS concentration (*18*). In contrast, the present study found that the encapsulation efficiency had a positive linear relationship with the increased CS concentration. This may be explained by the differences in chemical structure and molecular masses between BSA and tea catechins. As a macromolecule, protein has a complex three-dimensional conformation. The highly viscous nature of the gelation medium easily hindered the transfer of the BSA, whereas the tea catechin molecules, with one-dimensional conformation and small molecular mass (200−500 kDa), were structurally simpler than the protein molecule, which could easily escape from the encapsulation. Therefore, the highly viscous CS solution could prevent the tea catechin molecules from escaping the encapsulation of CS molecules, leading to a greater encapsulation efficiency.

The release kinetics and the total release of tea catechins in CS-TPP nanoparticles at isothermal conditions (37 °C) decreased with increasing CS concentration (**Figure 6C**). The release profile of the CS-TPP nanoparticles was affected by the encapsulation efficiency and the structure of CS-TPP nanoparticles influenced by CS molecular mass, deacetylation degree, CS concentration,

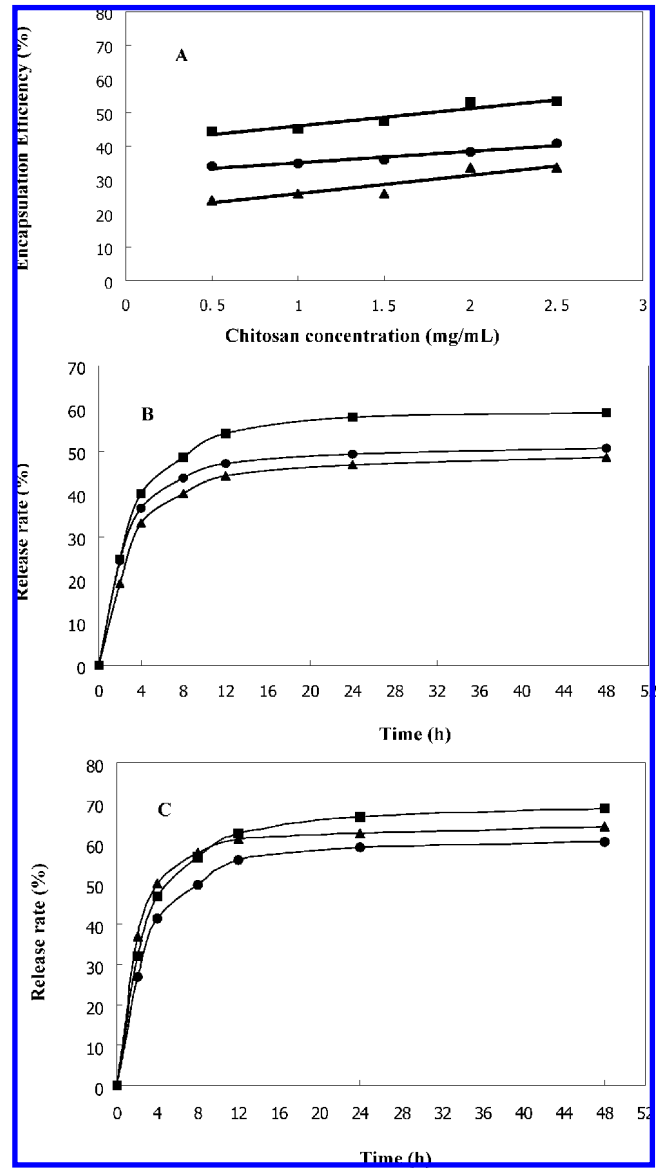

Figure 6. Effect of CS concentration (**A**) and CS molecular mass (**B**) (50 kDa,▲; 150 kDa, ■; and 300 kDa, ●) on the encapsulation efficiency and release in vitro of tea catechins. (CS-TPP mass ratio = 5:1; concentration of tea catechins = 1.0 mg/mL; pH 4.5.) Effect of CS concentration (0.5 mg/mL, ■; 1.5 mg/mL, ▲; and 2.5 mg/mL, ●) on subsequent tea catechins release profile (**C**). (CS molecular mass = 150 kDa; CS-TPP mass ratio = 5:1; concentration of tea catechins = 1.0 mg/mL, T = 37 °C).

and the CS/TPP mass ratio (*27*). **Figure 6C** indicates a higher encapsulation capacity with a lower release rate, suggesting that the CS concentration was more important than the encapsulation capacity. A similar result has also been reported by Xu et al. (*27*). As mentioned above, higher CS concentration led to larger nanoparticles (**Figure 1B**) and higher surface charge (**Figure 1C**). Tea catechin molecules were likely to bind to larger CS-TPP nanoparticles at multiple sites (*18*). In addition, membrane permeability of the CS nanoparticles would be theoretically lower with increasing CS concentration due to increased chain packing and rigidity, as well as interchain bonding. All of the above factors resulted in reduced burst effect and a slower release kinetic of the tea catechins. There was also a dramatic reduction in tea catechin release after 12 h, which is longer than that of protein (about 6 h) (*18*). It might also contribute to the small and simple molecular structures of tea catechins.

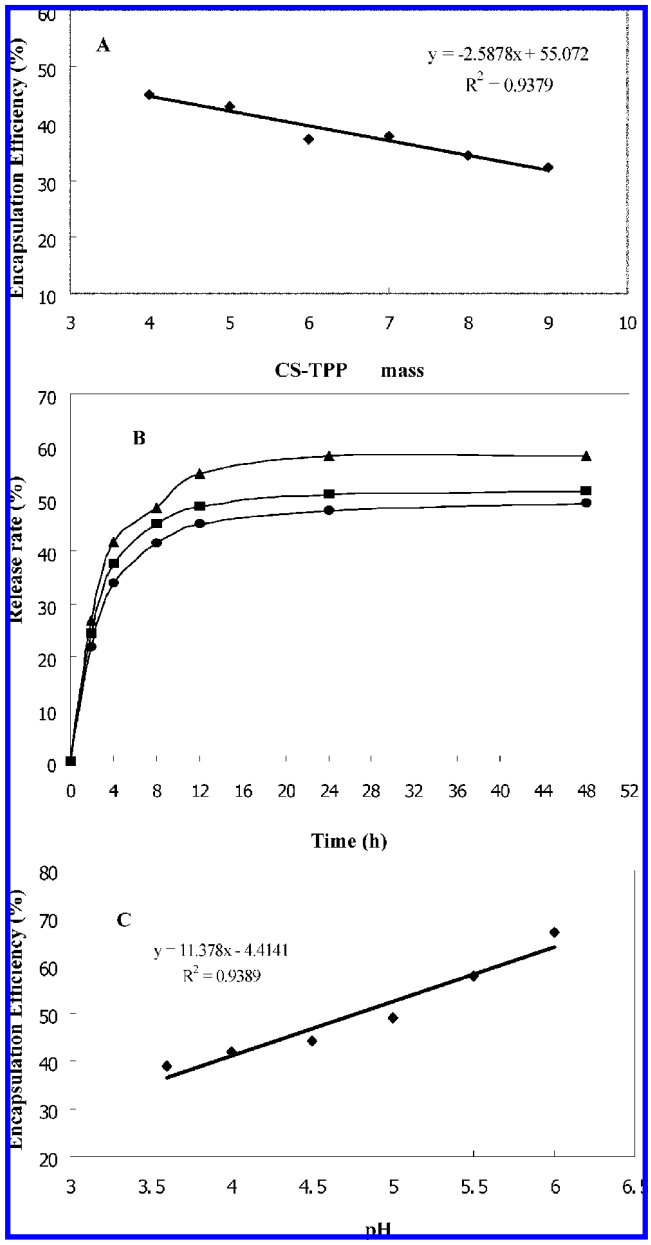

Figure 7. Effect of CS-TPP mass ratio (8:1, ●; 6:1, ■; and 4:1, ▲) on encapsulation efficiency (**A**) and release profile of tea catechin-loaded CS-TPP nanoparticles (**B**). (CS molecular mass = 150 kDa; CS concentration = 1.0 mg/mL; concentration of tea catechins = 1.0 mg/mL; pH 4.5, T = 37 °C.) Effect of CS solution pH on encapsulation efficient of catechin-loaded CS nanoparticles (**C**). (CS molecular mass = 150 kDa; CS concentration = 1.0 mg/mL; CS-TPP mass ratio = 5:1).

Effect of CS-TPP Mass Ratio. The effect of CS-TPP mass ratio on the encapsulation efficiency was studied at the mass ratios of 4:1, 5:1, 6:1, 7:1, 8:1, and 9:1 with 150 kDa CS. As shown in **Figure 7A**, the encapsulation efficiency of tea catechins decreased linearly from 45.14 to 32.23% as the CS-TPP mass ratio increased. This is consistent with that of BSA as target molecule in CS-TPP nanoparticles (*18*).

Tea catechin release kinetics and the total release at isothermal conditions decreased with the increase of CS-TPP mass ratio from 4:1 to 8:1 (**Figure 7B**). As the CS-TPP mass ratio decreased from 8:1 to 4:1, total release of tea catechins at 12 h increased from 45.16 to 54.81%. This phenomenon might be also reflected in the higher encapsulation efficiency of tea catechins at lower CS-TPP mass ratio. This result is consistent with the observation of BSA release in CS-TPP nanoparticles (*18*).

Effect of Initial pH Value of CS Solution. The encapsulation efficiency of tea catechins with the varying initial pH values of CS solution was investigated at pH 3.6, 4.0, 4.5, 5.0, 5.5, and 6.0. As shown in **Figure 7C**, the encapsulation efficiency of tea catechins increased linearly from 38.96 to 66.96% with the increasing initial pH values of CS solution. However, it was observed that precipitation would occur soon after the formation of nanoparticles prepared at pH 6.0, which might be caused by the relatively weak interaction between CS and TPP. Consistent with a previous paper (*29*), the present result suggests that it is possible to obtain relatively higher entrapment efficiency of the target molecule by careful control of the pH.

Effect of Concentration of Tea Catechins. Similar to previous studies (*18, 25*), a correct linear pertinence between the concentration of tea catechins and the size of the formed nanoparticles was observed (data not shown). Interestingly, the mean diameter of the CS-TPP nanoparticles loaded with tea catechins was smaller ($P < 0.01$) than that of the corresponding CS-TPP nanoparticles, which may be attributable to a greater cross-linking density of the tea catechin-loaded nanoparticles caused by the interactions between the CS matrix and tea catechins (*20*). No significant variations in zeta potential and PDI could be observed, which were centered at +33.8 mV and 0.203, respectively.

FT-IR. The FT-IR spectra of CS, CS-TPP nanoparticles, and CS-TPP nanoparticles loaded with tea catechins are shown in **Figure 5**. It should be noted that there were three characterizing regions between 3300 and 3500 cm^{-1}, between 1500 and 1700 cm^{-1}, and between 1000 and 1100 cm^{-1}, respectively. The cross-linking between CS and TPP and the interactions between tea catechins and CS-TPP nanoparticles were identified with FT-IR spectroscopy.

The peak between 3300 and 3450 cm^{-1} corresponds to the stretching vibration of hydroxyl, amino, and amide groups in CS (*25*). It could be noted that the peak at 3447.38 cm^{-1} in CS shifted to a lower wavenumber (3394.40 cm^{-1}) in CS-TPP nanoparticles, indicating that the interactions among these groups and TPP were also due to hydrogen bonding. Furthermore, a more obvious variation of this peak could be seen after loading with tea catechins. The peak shifted down to 3351.75 and flattened in the tea catechin-loaded particles compared with the corresponding CS-TPP nanopartcles, possibly due to the interactions of tea catechins with the non-cross-linked amino groups in CS.

Another essential change took place in the range of 1500 and 1700 cm^{-1}. The shifts of the 1643.00 and 1600.62 cm^{-1} peaks in CS to 1621.32 and 1560.94 cm^{-1}, respectively, in CS-TPP nanoparticles might be caused by the linkage between phosphate and ammonium ion, which reflected that the $-CONH_2$ and $-NH_2$ groups of CS were both cross-linked with TPP molecules. A similar result has been reported by Zhang and Kosaraju (*20*). However, the peak at 1621.32 cm^{-1} ($-CONH_2$) shifted to 1617.44 cm^{-1} for CS-TPP nanoparticles loaded with tea catechins, whereas the peak at 1560.94 cm^{-1} (N−H bending) almost remained the same (1561.02 cm^{-1}). This phenomenon indicates the presence of minor interactions between the hydroxyl groups in tea catechins and the amide group in CS nanoparticles.

The last but not the least region was between 1000 and 1100 cm^{-1}. The peak of 1083.21 cm^{-1} in theCS-TPP nanoparticles shifted to 1079.38 cm^{-1} in tea catechin-loaded CS-TPP nanoparticles. This peak is related with the symmetric stretch of C−O−C (*30*). The interaction between CS matrix and tea

catechins should lead to the shift of this peak in tea catechin-loaded CS-TPP nanoparticles.

In conclusion, CS-TPP nanoparticles and CS-TPP nanoparticles loaded with tea catechins were successfully prepared via the ionic gelation method. It is concluded that the formation of desirable CS-TPP nanoparticles and CS-TPP nanoparticles loaded with tea catechins is possible by controlling the critical fabricating parameters including CS molecular mass, CS concentration, and CS-TPP mass ratio.

LITERATURE CITED

(1) Higdon, J. V.; Frei, B. Tea catechins and polyphenols: health effects, metabolism, and antioxidant functions. *Crit. Rev. Food Sci. Nutr.* **2003**, *43*, 89–143.

(2) Kuzuhara, T.; Suganuma, M.; Fujiki, H. Green tea catechin as a chemical chaperone in cancer prevention. *Cancer Lett.* **2008**, *261*, 12–20.

(3) Baba, S.; Osakabe, N.; Natsume, M.; Muto, Y.; Takizawa, T.; Terao, J. In vivo comparison of the bioavailability of (+)-catechin, (−)-epicatechin and their mixture in orally administered rats. *J. Nutr.* **2001**, *131*, 2885–2891.

(4) Catterall, F.; King, L. J.; Clifford, M. N.; Ioannides, C. Bioavailability of dietary does of ^{3}H-labelled tea antioxidants (+)-catechin and (−)-epicatechin in rats. *Xenobiotica* **2003**, *33*, 743–753.

(5) Cai, Y.; Anavy, N. D.; Chow, H. S. S. Contribution of presystemic hepatic extraction to the low oral bioavailability of green tea catechins in rats. *Drug Metab. Dispos.* **2002**, *30*, 1246–1249.

(6) Nakagawa, K.; Ninomiya, M.; Okubo, T.; Aoi, K.; Juneja, L. R.; Kim, M.; Yamanaka, K.; Miyazawa, T. Tea catechin supplementation increases antioxidant capacity and prevents phospholipid hydroperoxidation in plasma of humans. *J. Agric. Food Chem.* **1999**, *47*, 3967–3973.

(7) Rinaudo, M. Chitin and chitosan: properties and applications. *Prog. Polym. Sci.* **2006**, *31*, 603–632.

(8) Bowman, K.; Leong, K. W. Chitosan nanoparticles for oral drug and gene delivery. *Int. J. Nanomed.* **2006**, *1*, 117–128.

(9) Agnihotri, S. A.; Mallikarjuna, N. N.; Aminabhavi, T. M. Recent advances on chitosan-based micro- and nanoparticles in drug delivery. *J. Controlled Release* **2004**, *100*, 5–28.

(10) Gan, Q.; Wang, T.; Cochrane, C.; McCrron, P. Modulation of surface charge, particle size and morphological properties of chitosan−TTP nanoparticles intended for gene delivery. *Colloids Surf. B* **2005**, *44*, 65–73.

(11) Kawashima, Y.; Handa, Y.; Takenaka, H.; Lin, S. Y.; Ando, Y. Novel method for the preparation of controlled-release theophylline granules coated with a polyelectrolyte complex of sodium polyphosphate−chitosan. *J. Pharm. Sci.* **1985**, *74*, 264–268.

(12) Lee, S. T.; Mi, F. L.; Shen, Y. J.; Shyu, S. S. Equilibrium and kinetic studies of copper ion uptake by chitosan−tripolyphosphate chelating resin. *Polymer* **2001**, *42*, 1879–1892.

(13) Shu, X. Z.; Zhu, K. J. A novel approach to prepare tripolyphosphate/chitosan complex beads for controlled release drug delivery. *Int. J. Pharm.* **2000**, *201*, 51–58.

(14) Panyam, J.; Labhasetwar, V. Biodegradable nanoparticles for drug and gene delivery to cells and tissue. *Adv. Drug Deliver. Rev.* **2003**, *55*, 329–347.

(15) Gåserød, O.; Jolliffe, A. G.; Hampson, F. C.; Dettmar, P. W. S.; Kjåk-Bræk, G. The enhancement of the bioadhesive properties of calcium alginate gel beads by coating with chitosan. *Int. J. Pharm.* **1998**, *175*, 237–246.

(16) Smith, J.; Wood, E.; Dornish, M. Effect of chitosan on epithelial cell tight junctions. *Pharm. Res.* **2004**, *21*, 43–49.

(17) Panyam, J.; Zhou, W. Z.; Prabha, S.; Sahoo, S. K.; Labhasetwar, V. Rapid endo-lysosomal escape of poly(D,L-lactide-*co*-glycolide) nanoparticles: implications for drug and gene delivery. *FASEB J.* **2002**, *16*, 1217–1226.

(18) Gan, Q.; Wang, T. Chitosan nanoparticle as protein delivery carrier—systematic examination of fabrication conditions for efficient loading and release. *Colloids Surf. B* **2007**, *59*, 24–34.

(19) Tsai, M. L.; Bai, S. W.; Chen, R. H. Cavitation effects versus stretch effects resulted in different size and polydispersity of ionotropic gelation chitosan−sodium tripolyphosphate nanoparticle. *Carbohydr. Polym.* **2008**, *71*, 448–457.

(20) Zhang, L.; Kosaraju, S. L. Biopolymeric delivery system for controlled release of polyphenolic antioxidants. *Eur. Polym. J.* **2007**, *43*, 2956–2966.

(21) Calvo, P.; Remunan-Lopez, C.; Vila-Jato Alonso, M. J. Novel hydrophilic chitosan−polyethylene oxide nanoparticles as protein carrier. *J. Apply. Polym. Sci.* **1997**, *63*, 125–132.

(22) Nurmi, K.; Ossipov, V.; Haukioja, E. Variation of total phenolic content and individual low-molecular-weight phenolichitosan in foliage of mountain birch trees (*Betula pubescens* ssp *tortuosa*. *J. Chem. Ecol.* **1996**, *22*, 2023–2040.

(23) Zhou, B.; Wang, L.; Li, W.; Sun, Y.; Ye, H.; Zeng, X. Isolation of methylated catechins from tea and their analysis by high performance liquid chromatography. *Chinese J. Anal. Chem* **2008**, *36*, 494–498.

(24) Floury, J.; Desrumaus, A.; Axelos, M. A. V.; Legrand, J. Degradation of methylcellulose during ultra-high pressure homogenization. *Food Hydrocolloids* **2002**, *16*, 47–53.

(25) Wu, Y.; Yang, W.; Wang, C.; Hu, J.; Fu, S. Chitosan nanoparticles as a novel delivery system for ammonium glycyrrhizinate. *Int. J. Pharm.* **2005**, *295*, 235–245.

(26) Grenha, A.; Seijo, B.; Remuñán-López, C. Microencapsulated chitosan nanoparticles for lung protein delivery. *Eur. J. Pharm. Sci* **2005**, *25*, 427–437.

(27) Xu, Y. M.; Du, Y. M. Effect of molecular structure of chitosan on protein delivery properties of chitosan nanoparticles. *Int. J. Pharm.* **2003**, *250*, 215–226.

(28) Papadimitriou, S.; Bikiaris, D.; Avgoustakis, K.; Karavas, E.; Georgarakis, M. Chitosan nanoparticles loaded with dorzolamide and pramipexole. *Carbohydr. Polym.* **2008**, *73*, 44–54.

(29) Müller, R. H.; Jacobs, C.; Kayser, O. Nanosuspensions as particulate drug formulations in therapy rationale for development and what we can expect for the future. *Adv. Drug Deliver. Rev.* **2001**, *47*, 3–19.

(30) Banerjee, T.; Mitra, S.; Kumar, S. A.; Kumar, S. R.; Maitra, A. Preparation, characterization and biodistribution of ultrafine chitosan nanoparticles. *Int. J. Pharm.* **2002**, *243*, 93–105.

Received for review April 8, 2008. Revised manuscript received June 11, 2008. Accepted June 11, 2008. This work was supported by a grant-in-aid from 863 Program, Ministry of Science and Technology, People's Republic of China (2007AA10Z351 and 2007AA100403) and a grant-in-aid from Nanjing Agricultural University for the Introduction of Outstanding Scholars (804066).

JF801111C